Engineering robust control of two-component system phosphotransfer using modular scaffolds

Weston R. Whitaker[a,b], Stephanie A. Davis[c], Adam P. Arkin[b,d,e,1], and John E. Dueber[b,d,e,1]

[a]The University of California, Berkeley and University of California, San Francisco Graduate Program in Bioengineering, Berkeley, CA 94720; Departments of [b]Bioengineering, and [c]Chemistry, University of California, Berkeley, CA 94720; [d]Physical Biosciences Division, Lawrence Berkeley National Laboratory, Berkeley, CA 94720; and [e]Energy Biosciences Institute, University of California, Berkeley, CA 94720

Edited by Thomas J. Silhavy, Princeton University, Princeton, NJ, and approved September 19, 2012 (received for review June 1, 2012)

Synthetic biology applies engineering principles to facilitate the predictable design of biological systems. Biological systems composed of modular parts with clearly defined interactions are generally easier to manipulate than complex systems exhibiting a large number of subtle interactions. However, recreating the function of a naturally complex system with simple modular parts can increase fragility. Here, inspired by scaffold-directed signaling in higher organisms, we modularize prokaryotic signal transduction to allow programmable redirection of phosphate flux from a histidine kinase to response regulators based on targeting by eukaryotic protein–protein interaction domains. Although scaffold-directed colocalization alone was sufficient to direct signaling between components, this minimal system suffered from high sensitivity to changing expression levels of each component. To address this fragility, we demonstrate how to engineer autoinhibition into the kinase so that phosphotransfer is possible only upon binding to the scaffold. This system, in which scaffold performs the dual functions of activating this autoinhibited kinase and directing flux to the cotargeted response regulator, was significantly more robust to varying component concentrations. Thus, we demonstrate that design principles inspired by the complex signal-transduction pathways of eukaryotes may be generalized, abstracted, and applied to prokaryotes using well-characterized parts.

protein engineering | signaling specificity | protein scaffolds

Living cells exhibit a remarkable ability to process multiple signals to maintain homeostasis in a dynamic environment, to diversify or specialize behavior, and to organize complex structures. Signal-transduction pathways (STPs) play a key role in these processes as essential elements in sensing, processing, and transmitting environmental information, often at rapid speeds and with the potential to hold different states at different locations within the same cell. As synthetic biology is challenged to design more sophisticated systems, it will become increasingly important to match these abilities in a designable and predictable manner. Impressive successes toward these goals have been made in the design of genetic circuits, achieving a diverse set of desired behaviors by varying the arrangement of common transcriptional regulators and promoters (1–4). The physical and functional modularity of genes and promoters is essential for allowing parts to be rearranged easily with relatively predictable behavior (5). Although connectivity at the transcriptional level can be rewired via adjacency on DNA, connectivity of STPs generally is determined through interactions among many interface residues that are difficult to manipulate with predictable behavior. One recent study, however, successfully engineers modular control into the yeast mating STP through colocalization of positive or negative signaling modulators to the Ste5 scaffold via introduced binding domains (6). By rearranging the recruitment machinery to alter the feedback acting on the pathway, an impressive range of sophisticated temporal and steady-state behavior is achieved.

Eukaryotic signaling-pathway proteins often are composed of a catalytic output domain regulated by physically distinct input domains (7). Domain-recombination events allow novel input/output linkages as well as reshaping the transfer function of a given signaling response (8, 9). Scaffolds, which organize catalytic activities spatially, represent an extreme example of the evolutionary benefits of input modularity by allowing catalysis and input control to be separated into distinct molecules (10, 11). Prokaryotic organisms, however, make far less extensive use of such modular organization, with the notable exception of CheW in the chemotaxis complex, which already has demonstrated utility in synthetic biology applications (12). Generally, prokaryotic signaling proteins encode both catalytic activity and binding specificity into the same cooperative fold. This dual encoding raises the question of whether engineering strategies mimicking eukaryotic modular organization would be effective for directing signaling flux in the form of phosphate transfer in prokaryotes.

Two-component systems (TCSs) represent an attractive target for engineering signal transduction because they are the predominant signaling strategy used by prokaryotes for sensing a wide array of environmental signals, have a well-characterized, conserved phosphotransfer scheme (13), and have highly conserved phosphotransfer structures (14), suggesting that lessons learned from one pathway could be applied to many others. The TCS signal-transduction architecture generally is organized around two conserved proteins, a histidine kinase (HK) that senses a stimulus and autophosphorylates and a response regulator (RR) to which the phosphate is transferred. RRs subsequently actuate a response, usually transcriptional regulation. Phosphotransfer routing and the coupling of stimulus to activity are both important aspects of signal transduction, but in this work we focus primarily on the former. In the last decade, significant progress has been made in understanding TCS phosphotransfer routing and the precise mechanisms by which phosphotransfer specificity is encoded in TCS (15–18). In particular, although detectable phosphotransfer cross-talk between noncognate components is somewhat common for purified components in vitro (19), a clear kinetic preference for phosphotransfer between cognate pairs appears to be a major determinant of specificity (16). We propose that TCS kinetic preference is the result, at least in part, of specific binding (i.e., a K_m effect), and therefore an increased local concentration through the synthetic assembly of HK and RR substrate could serve as a basis for controlling signaling for noncognate components. The degree to which the local concentration controls flux in the scaffolded pathways of higher organisms is unclear,

Author contributions: W.R.W., A.P.A., and J.E.D. designed research; W.R.W. and S.A.D. performed research; W.R.W., S.A.D., A.P.A., and J.E.D. analyzed data; and W.R.W., A.P.A., and J.E.D. wrote the paper.

The authors declare no conflict of interest.

This article is a PNAS Direct Submission.

[1]To whom correspondence may be addressed. E-mail: aparkin@lbl.gov or jdueber@berkeley.edu.

This article contains supporting information online at www.pnas.org/lookup/suppl/doi:10.1073/pnas.1209230109/-/DCSupplemental.

but the frequency of enzyme coassembly suggests it does play a significant role. Interestingly, recent work also has identified HKs containing domains responsible for binding RRs that may play a role in determining kinase specificity (20, 21). In this work we replace several native TCSs with components that have been translationally fused to protein–protein interaction domains and peptide ligands, so that expression of synthetic scaffolds can be used specifically to colocalize noncognate components for the purpose of directing phosphotransfer in vivo.

Results

Colocalization Amplifies Weak Natural Cross-Talk. We have designed an in vivo assay to examine phosphotransfer specificity consisting of one HK exhibiting weak natural cross-talk to two noncognate RRs. In vitro phosphotransfer assays show that although some cross-talk to one or a few noncognate RRs is common for most HKs, EnvZ appears to phosphotransfer to a particularly large number of noncognate RRs (16, 19). Additionally, the large number of studies on Taz, a HK chimera of the Tar-sensing domain and the EnvZ cytoplasmic domain that gives the phosphotransfer specificity of EnvZ but with a more well-defined input control (22), led us to choose Taz as our model HK. To study the phosphotransfer specificity in vivo, Taz, as well as noncognate RRs, were expressed on independent, inducible promoters, and fluorescent transcriptional reporters for both target RRs were introduced on a plasmid (see Dataset S1 for a summary of plasmids and Fig. S1 for examples of plasmid schematics). Cross-talk between EnvZ and CpxR has been well characterized (17, 23), making it an obvious choice for targeted cross-talk. Additionally, EnvZ exhibits in vitro cross-talk to CusR (16). Overexpression of Taz was sufficient to detect increased CusR and CpxR reporter activity even in an *Escherichia coli* strain containing the native TCSs (Fig. S2). Removing the native pathways led to further increased Taz-CpxR and Taz-CusR cross-talk, displaying significant Taz-dependent activation of RRs at lower Taz expression levels (Fig. S2), as would be expected from removing competitive binding and phosphotransfer buffering from native components (24, 25).

To amplify the low level of noncognate cross-talk (Fig. 1*A*) in a controllable manner, we translationally fused protein–protein interaction domains to the TCSs to increase local concentrations and thus phosphotransfer rates. Although a large number of domains are available for this purpose (26, 27) we chose the Crk SH3 domain and ligand because of its independent folding, tight affinity [as low as K_d = 100 nM (28)], and successful use in previous synthetic biology applications (8, 29, 30). Rather than attempting to control component orientation precisely, the domain or ligand was fused to the C terminus of the HK or RR, respectively, with linkers composed of 12 residues of glycine and serine. These linkers are predicted to be unstructured and flexible; thus the engineered assembly is designed solely for the purpose of increasing the local concentration of colocalized components. At low expression levels of Taz and CpxR, reporter activation can be seen only in the presence of engineered interaction(s) between SH3-fused Taz and ligand-fused CpxR (Fig. 1*B*). As the number of binding domains fused to Taz and as the affinity of the peptide ligand increases, the reporter fluorescence, and thus the phosphorylation of CpxR, also increase (Fig. 1*B*). Results similar to Taz/CpxR were observed for SH3-dependent Taz/CusR recruitment (Fig. S3*A*). (All ligand affinities refer to reported in vitro affinities between free ligand and domain and do not include fusions to TCSs.) In addition to amplifying noncognate signaling in strains lacking native components, colocalization also overcame native pathway buffering at higher expression levels of components (Fig. S3 *B* and *C*), particularly when native pathways are acting primarily as phosphatases, as is the case for CusR's native HK, CusS (Fig. S3*B*). These results are consistent with our hypothesis that a local concentration effect can be used to increase phosphotransfer rates between otherwise weakly cross-talking TCS pairs. Further supporting this hypothesis, noncognate phosphotransfer was increased in a reconstituted system with purified HK, RR, and scaffold (Fig. S3*D*).

Synthetic Scaffolding Directs Histidine Kinase Specificity. Scaffold proteins were designed to recruit either CusR or CpxR to Taz, allowing Taz specificity to be redirected through the expression

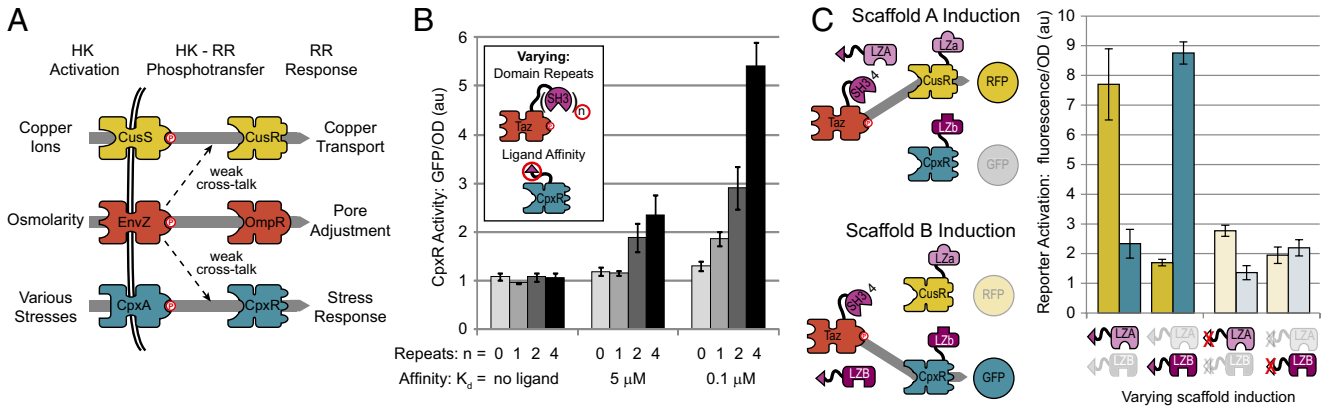

Fig. 1. Phosphotransfer to a noncognate response regulator can be directed by synthetic assembly with an HK. (*A*) Highly specific natural TCSs exhibit weak phosphotransfer cross-talk to noncognate RRs. (*B*) The effect of SH3 domain/ligand-directed colocalization between Taz and CpxR was measured in cells via CpxP promoter-driven GFP and normalized so that background cell autofluorescence measures 1 arbitrary unit (au). Error bars represent SE from three independent experiments. Taz was expressed with 0, 1, 2, or 4 SH3 domains tethered by repeating glycine/serine flexible linkers. CpxR was expressed fused either to no ligand, a single weak-affinity (in vitro reported K_d = 5 μM) ligand, or a single tight-affinity (in vitro reported K_d = 0.1 μM) ligand. (*C*) Scaffolds were composed of an SH3 peptide fused to one of two different leucine zippers, LZA or LZB, each specific to a corresponding leucine zipper, LZa or LZb, fused respectively to CusR or CpxR. Taz-$(SH3)_4$, CusR-LZa, and CpxR-LZb were expressed at constant levels. Scaffolds for phosphotransfer to CusR or CpxR were encoded genetically in one strain under salicylate- or anhydrous tetracycline (aTc)-inducible control, respectively. Another strain similarly expressed both nonfunctional scaffolds with mutations that severely reduce SH3 binding. Inductions of the two scaffolds were varied, and CpxR-driven GFP and CusR-driven RFP were measured for the strain with functional scaffold (dark blue and dark yellow) and for the strain with nonfunctional scaffold (light blue and light yellow). High RFP and GFP signal was observed only with induction of the corresponding functional scaffold.

of different scaffolds (Fig. 1*C*). Each scaffold contained an SH3 peptide ligand, targeting it to Taz-$(SH3)_4$, a Taz that has been fused to four SH3 domains, each of which was separated by 12-residue glycine/serine linkers. Each scaffold additionally includes one of two different synthetic leucine zippers fused to the SH3 peptide with a nine-residue glycine/serine linker. Leucine zippers were chosen because of the large number of available high-affinity pairs (31, 32) and their successful use in previous synthetic biology applications (6, 33). Each scaffold leucine zipper (here termed "LZA" and "LZB") incorporated into the scaffold was specific for a corresponding zipper, LZa and LZb, that was fused to either CusR or CpxR, respectively, with a 10- or 12-residue glycine/serine linker. Taz-$(SH3)_4$, CusR-LZa, and CpxR-LZb were expressed simultaneously at constant levels, whereas the expression of the two scaffolds, SH3pep-LZA and SH3pep-LZB, were induced as indicated. To monitor pathway flux, CusR and CpxR reporters driving RFP and GFP expression, respectively, were used. Fig. 1*C* shows alternating expression between scaffolds redirects specificity of the HK; reporter activation occurs only when the scaffold capable of colocalization to the HK is expressed. Scaffolds also were made with point mutations that changed the PxxP motif in the SH3 peptide to AxxA, which severely decreases affinity for the SH3 domain (34). As expected, these scaffolds exhibited substantially diminished function (Fig. 1*C*). Switching expression between the functional scaffolds resulted in a 17-fold change in the ratio of RFP/OD to GFP/OD [56-fold with background autofluorescence, i.e., 1 arbitrary unit (au), subtracted], showing that, even with long, flexible linkers, colocalization can influence phosphotransfer signaling rates dramatically.

Scaffold-Dependent Control of Specificity Is Sensitive to Component Concentration. Achieving scaffold-directed control of phosphotransfer required careful optimization of the expression of each signaling component. To investigate this dependency, expression levels were varied for both the HK, Taz-$(SH3)_4$, and RR, CusR, either with or without an SH3 peptide for colocalization. Three expression levels, representing low (*i*), moderate (*ii*), and high (*iii*) induction levels are plotted in Fig. 2*A*. Colocalization produced a large increase in signaling only at moderate induction. To illustrate the concentration regime in which colocalization was effective, the fold change in reporter activity with and without SH3 peptide fused to CusR is plotted for each HK and RR induction level (see Dataset S1 for individual fluorescent values). As expected from Fig. 1*B*, colocalization via direct recruitment substantially increased signaling, but this effect was observed only within a limited range of HK and RR concentrations (Fig. 2*B*). This sensitivity to component concentrations is consistent with the hypothesis that phosphotransfer is modulated by local concentration.

Scaffold concentrations also must be optimized to achieve efficient corecruitment of HK and RR. As scaffold induction is increased, we expect activity to display a biphasic behavior, initially increasing up to a maximum and then decreasing as excess scaffold competition for components results in sequestration of pathway components (i.e., fewer ternary complexes of scaffold:HK:RR), as predicted for scaffolding of MAP kinase STPs (35) and experimentally verified specifically for the Ste5 scaffold (36). We tested this prediction in our system with constant expression of Taz-$(SH3)_4$ and CpxR-LZb while SH3pep-LZB scaffold was induced to different levels. As predicted, CpxR activation initially increased as scaffold expression was induced, but a maximum effect was reached, after which further scaffold expression resulted in a decrease in CpxR reporter fluorescence (Fig. 2*C*). Western blots of epitope-tagged constructs confirm that scaffold concentrations exceeding component concentrations correspond with decreased signaling (Fig. S4 *B* and *C*). Thus, achieving nearly maximal scaffold-dependent signaling required carefully balanced scaffold:targeted protein concentrations.

Engineering Autoinhibition for Scaffold-Dependent Activation of HK. Robustness is a critical feature of natural TCSs, ensuring that, despite variation in component concentration, specificity is maintained so that the sensory machinery acts on the correct target

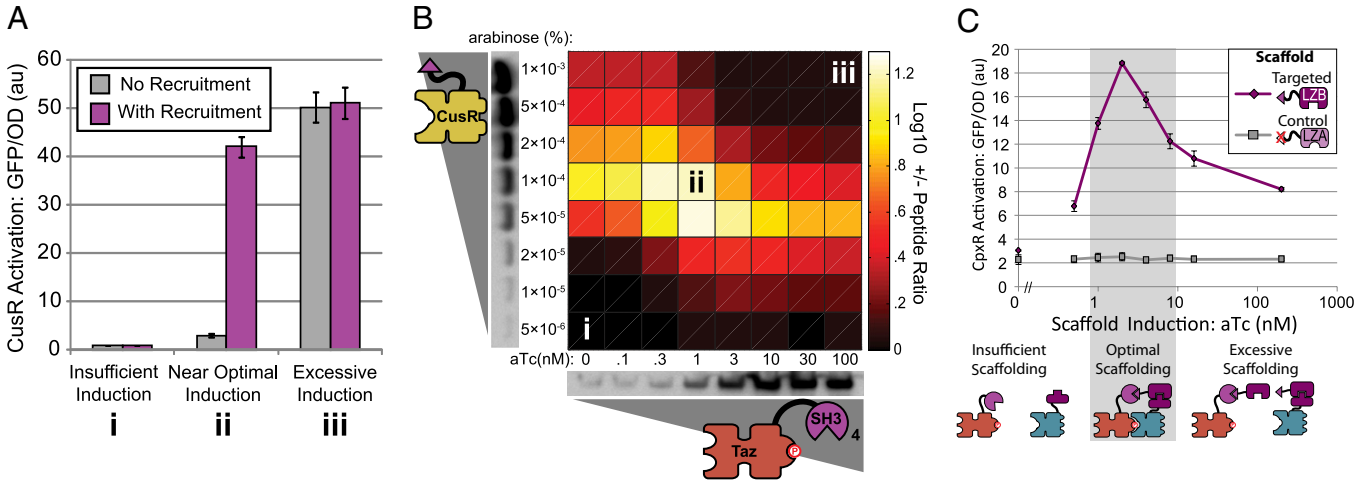

Fig. 2. Colocalization-controlled phosphotransfer is sensitive to component concentrations. (*A*) Expression of Taz-$(SH3)_4$ was titrated with the aTc-inducible promoter, P_{tet}, and expression of CusR both with and without SH3 peptide fusion was titrated with the arabinose-inducible promoter, P_{BAD}. Representative conditions including underexpression, nearly optimal expression, and overexpression of components are marked (*i*), (*ii*), and (*iii*), respectively. (*B*) Expanding on plot *A*, for each induction level the ratio representing the corecruitment effect was calculated by dividing the GFP/OD measured for CusR with SH3 peptide by that measured without SH3 peptide fusion, with a maximal 17-fold increase in GFP/OD with peptide addition. To estimate relative concentrations of components, Western blots of epitope-tagged HK and RR versions (Fig. S4*A*) are included along the axes. (*C*) Taz-$(SH3)_4$ and CpxR-LZb were expressed at a constant level while scaffold expression from the P_{tet} promoter was varied via aTc titration. As induction of scaffold designed to colocalize Taz and CpxR was increased, CpxR activity displayed a biphasic response, giving a maximum efficiency at an intermediate scaffold concentration. As induction of a control scaffold (not capable of colocalizing CpxR or Taz) was increased, CpxR activity remained low, as expected.

RR, and that the RR is set to the phosphorylation level appropriate for the stimulus. Natural TCSs meet these goals primarily through high-kinetic preference of the HK for cognate RRs (16) and bifunctional—kinase and phosphatase—activities (15, 37). We have added the additional goal of scaffold-dependent control of phosphotransfer (Fig. 1*C*), but Fig. 2 shows that this quality was not robust to changes in component concentrations. In natural eukaryotic systems, in addition to localizing components, scaffolding can serve to activate components, e.g., in the activation and localization of the Ras kinase by the KSR scaffold in the mammalian ERK pathway (38). Combining activation and assembly should prevent undesired signaling in the absence of scaffolding. We have engineered autoinhibition of Taz kinase activity by adding an intramolecular SH3/ligand interaction similar to that seen in many eukaryotic signaling proteins (8, 29, 39). In this design (Fig. 3*A*), the HK bore a ligand in addition to a flexibly linked SH3 scaffold domain. Intramolecular interaction of the SH3 domain with the ligand competitively inhibited activation of the RR until the intramolecular interaction was displaced by an intermolecularly supplied target peptide. This design ensured that high expression of autoinhibited Taz did not contribute to undesired activation of RRs in the absence of targeting of RR to the HK.

To engineer an intramolecular interaction, we tethered an SH3 domain to the C terminus of Taz and inserted an SH3 peptide ligand internally in the structure. The first aim was to introduce this peptide insertion without perturbing activity in the absence of the intramolecular interaction. As described in detail in *SI Materials and Methods* and shown in Fig. S5, we inserted the peptide flanked by a linker sequence of degenerate residues constrained to the polar/nonpolar pattern that would be expected to serve as a structured linker extending the four-helix bundle (Fig. 3*B* and Fig. S5 *A–C*). Linker library patterns first were screened in the absence of engineered colocalization for the ability to retain phosphotransfer activity to CusR at high Taz and CusR concentrations, so that colocalization was not required for signaling. One of the most promising candidates, AiTaz(29A), had an inserted high-affinity SH3 ligand [reported $K_d = 0.1$ μM measured *in trans* (28)] and with the fusion of four C-terminal SH3 domains displayed low basal activity (Fig. 3*C*). To verify that the degree of autoinhibition is determined by the affinity of the intramolecular SH3 interaction, we replaced the high-affinity peptide ($K_d = 0.1$ μM) with a lower-affinity peptide ($K_d = 5$ μM) and a nonfunctional peptide (AxxA) (34) to make switches AiTaz(29B) and AiTaz(29C), respectively. All three switches tested without SH3 domain fusions retained nearly wild-type activation of CusR, indicating that the structured linker for AiTaz(29A) could tolerate altered SH3 peptide length and sequence without disrupting kinase function (Table S1).

Scaffolds containing one nonfunctional, one high-affinity ($K_d = 0.1$ μM), or two high-affinity SH3 peptides were expressed to test scaffold-dependent activation of the autoinhibited Taz. The AiTaz(29B)-$(SH3)_4$ was activated by scaffolds with one or two SH3 high-affinity peptides, whereas the scaffold with two peptides, potentially through a cooperative multivalency effect, was considerably more effective at releasing autoinhibition of the AiTaz(29A)-$(SH3)_4$. The AiTaz(29C)-$(SH3)_4$, containing a nonfunctional peptide insertion and displaying no apparent autoinhibition, was not affected by scaffold expression. In these experiments (Fig. 3*C*), scaffold was used solely as an activator, because CusR did not have a tethered scaffold-targeting ligand. These results demonstrate that we have engineered an autoinhibited HK that exhibits scaffold-dependent activation.

Autoinhibition Improves Robustness of Scaffold-Directed Specificity. Scaffold-dependent HK activity should improve robustness to varying expression levels by lowering phosphotransfer in the absence of a synthetic assembly. To test a wide range of steady-state Taz concentrations, expression was driven with the P_{tet} promoter with either of two different strength ribosome-binding sites, allowing for a titration spanning more than a 400-fold range as approximated by Western blot intensity quantification (Fig. S4*D*). The scaffold consisted of two SH3 peptides, to target and activate AiTaz(29A)-$(SH3)_4$, as well as LZB to recruit CpxR-LZb. Without the incorporation of autoinhibition, scaffold expression significantly increased activation of the targeted CpxR-LZb at intermediate expression of Taz-$(SH3)_4$ (Fig. 4*A*). However, the fold change in activity driven by scaffold varied substantially as Taz expression was changed (Fig. 4*B*), consistent with previously characterized sensitivity to HK concentration (Fig. 2*B*). Particularly problematic was the activation of CpxR in the absence of scaffold when Taz expression levels are high. When autoinhibition was introduced, both with and without scaffold, a striking insensitivity to changes in Taz concentrations was shown: A fixed amount of pathway flux was achieved in the presence of scaffold, but only nearly background fluorescence was measured in the absence of scaffolding even as Taz expression was increased by over 400-fold (Fig. 4*A*). Expression of scaffold was capable of activating CpxR substantially even at very low AiTaz(29A)-$(SH3)_4$ expression levels (1.6–7.1 au) but activation was nearly absent (1.5–1.9 au) when the HK expression plasmid was replaced with a control vector. Although the maximum ratio of GFP/OD was similar with or without scaffold (Fig. 4*B* and Fig. S6*A*), at 6.5- and 5.9-fold, respectively, without and with autoinhibition (11- and 20-fold, respectively, with background fluorescence subtracted), the effect was far more sensitive to kinase expression levels in the absence of autoinhibition. Higher expression of scaffold further activates the autoinhibited

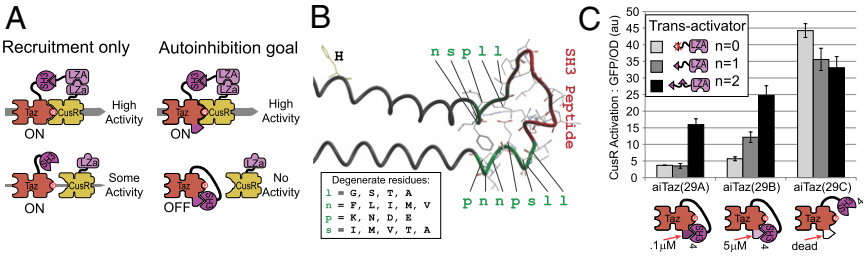

Fig. 3. Engineering scaffold-controlled activation of HK via a competitive autoinhibitory interaction to reduce nontargeted signaling. (*A*) To limit phosphotransfer in the absence of an engineered interaction, we introduced an autoinhibitory SH3 interaction, so that scaffold may both localize HK-RR and activate HK. (*B*) The sequence near the turn between helices of the four-helix bundle of the dimerization/phosphotransfer domain of Taz was targeted for peptide insertion. This sequence was replaced with a library that included an SH3 ligand flanked by a library of degenerate residues expected to continue the α-helixes of the four-helix bundle. A homology-based structure prediction, from the Phyre web server (45) for AiTaz(29A) is shown with degenerate residues labeled. (*C*) CusR, lacking any engineered interaction motifs, was highly expressed to test scaffold-dependent activation of HK in the absence of engineered colocalization. Activity of the Taz switches AiTaz(29A)-$(SH3)_4$, AiTaz(29B)-$(SH3)_4$, and AiTaz(29C)-$(SH3)_4$, containing SH3 ligands of high ($K_d = 0.1$ μM), intermediate ($K_d = 5$ μM), or nonfunctional (AxxA) affinity, respectively, were tested with scaffolds with various input ligand sequences. In the absence of functional transactivating peptide ($n = 0$), the activity of the HK decreased in a manner dependent on the affinity of the engineered interaction. Expression of scaffold containing one SH3 ligand peptide and especially two SH3 ligand peptides competitively activated the switch. See Table S1 for data on all combinations of kinases, number of fused domains, and identity of transacting peptide.

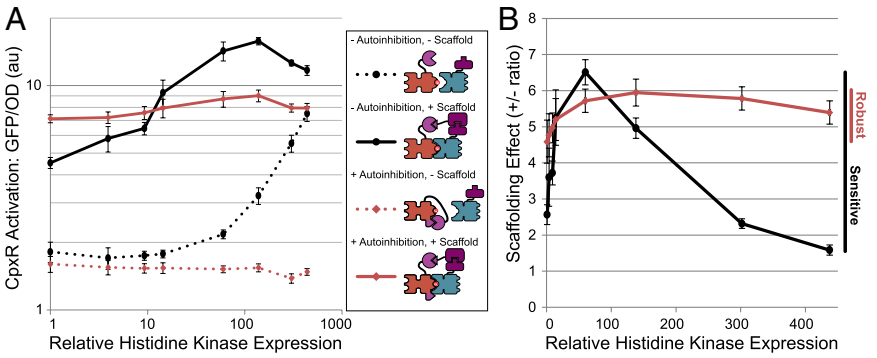

Fig. 4. Autoinhibition decreased sensitivity to HK concentrations. (*A*) Titration of HK concentrations across a >400-fold range was achieved by titrating the P_{tet} inducer, aTc, for two expression vectors including either a weak or strong RBS upstream of Taz-$(SH3)_4$ or AiTaz(29A)-$(SH3)_4$. Relative kinase concentrations, as estimated by Western blot densitometry (Fig. S4*D*), are plotted on the *x*-axis. CpxR-LZb was expressed at a constant level, and CpxR activity is measured via GFP/OD in the presence of Taz with and without autoinhibitory interaction as well as with and without $(SH3pep)_2$-LZB scaffold expression. In absence of autoinhibition, CpxR activation increased for the scaffolded assembly as HK concentrations were increased (solid black line). The system without scaffold also began to phosphotransfer but required higher HK expression levels (dotted black line). With the addition of autoinhibition, the GFP/OD remained at nearly background levels in the absence of scaffolding (dotted red line), even as the high-strength RBS construct was fully induced, and CpxR activation with scaffold expression (solid red line) also showed reduced variation. (*B*) The fold change in GFP/OD upon expression of scaffold is plotted for the systems with and without autoinhibition. The effect of scaffolding was far more variable in the system lacking autoinhibition, producing a high effect from scaffolding only at intermediate HK concentrations, whereas the scaffolding effect remained steady as the concentration of the autoinhibited HK was varied.

HK, increasing CusR (Fig. S6*B*) and CpxR (Fig. S6*C*) activation each by more than 10-fold (more than 25-fold with background fluorescence subtracted). These results show that, although we have increased the sophistication of a component in this system by incorporating the autoinhibitory interaction into Taz, we were able to reduce the complexity of the system response, because the device output was sensitive to fewer component concentrations. Rather than carefully balancing kinase concentrations to achieve scaffold-directed specificity, a wide range of autoinhibited kinase expression levels should be sufficient for achieving scaffold-mediated control, simplifying the design process for future applications.

Discussion

Here we have shown that, although TCS signaling components have not evolved to use scaffolding, synthetic scaffolds made from well-characterized, modular interaction domains can be used to control TCS specificity. Switching expression between two synthetic scaffolds was used to direct phosphate selectively from the Taz HK to either the CusR or the CpxR RR, depending on the identity of the scaffold expressed. Thus, the simple act of colocalizing signaling components, a primary function of most eukaryotic scaffolds, was sufficient to control phosphotransfer specificity of TCSs. However, scaffold-controlled phosphotransfer was highly sensitive to the expression level of each component. To reduce this sensitivity to differences in steady-state expression levels, we incorporated an autoinhibitory interaction into Taz so that the scaffold performs the dual roles of activating and colocalizing the kinase with its target, a characteristic found in natural scaffolded pathways (38, 40). It is possible that autoinhibited HK also may be more robust to temporal variation in component concentration, although investigation would require experiments with higher temporal resolution than the currently used transcriptional reporters. We expect the method of incorporating autoinhibition developed here will be broadly applicable to other HKs because it targets a highly conserved signaling structure. This work demonstrates that the design principles underlying the robust, but highly evolvable, signaling pathways in higher organisms may be generalized, abstracted, and applied to prokaryotes using well-characterized, modular signaling enzymes and protein–protein interaction domains.

Several recent advances should allow this scaffolding strategy to be applied generally to other TCSs. We have focused on two of the noncognate pairs shown to cross talk weakly in vitro: EnvZ-CpxR and EnvZ-CusR (16). Other noncognate pairs lacking detectable in vitro cross-talk also may lack physiologically relevant phosphotransfer rates even when coassembled. A solution may come from studies showing that mutations in the specificity-determining residues (17, 41) can be used to tune phosphotransfer rates and even increase HK promiscuity. Another challenge is that it is common, as was observed for both Taz/CusR and Taz/CpxR tested in this study, for noncognate pairs displaying cross-talk to display constitutive activity rather than coupling activity with stimulus, even when colocalized (Fig. S3 *E* and *F*). A recent study demonstrates a solution, showing that a series of mutations to CpxA can change a constitutive phosphotransfer interaction into a stimulus-dependent switch for phosphorylation of noncognate OmpR (15). These remarkable successes uncovering the mechanisms governing natural TCS signal transduction specificity provide a number of promising methods for tuning TCS components for engineering applications.

TCSs offer a promising means of developing sophisticated STPs. By encoding specificity with modular scaffolds, the large number of well-characterized orthogonal binding domains (27), some of which include additional control points such as light-induced binding, can be applied directly to controlling signaling specificity. Directing pathway output to protein localization, such as CheY-FliM phosphorylation-dependent localization, instead of transcription control could provide a powerful tool for actuating a wide variety of responses, even in higher organisms that would not respond directly to phosphorylated RR. Because protein localization can be both an input, as demonstrated here, and an output of TCS pathways, multiple scaffold-controlled pathways potentially can be linked for multilayer processing at fast time-scales. Although our system followed a canonical structure, with an HK directly phosphorylating the transcription-regulating RR, the application of scaffolding to create longer phosphotransfer relays, as seen in natural hybrid TCSs, is a promising extension, particularly if more sophisticated processing or additional control points are desired. The *Bacillus subtilis* sporulation pathway uses TCS phosphotransfer structures to build a sophisticated signal-transduction pathway with multiple points of feedback control (42). Multiple phosphotransfer steps also may offer an alternative to maintain stimulus sensitivity, in which the stimulus-dependent phosphorylation/dephosphorylation control could occur upstream, whereas constitutive phosphotransfer may be sufficient for downstream scaffold-controlled phosphotransfer routing. Phosphorelays built from TCS components offer a particularly promising direction for scaling to larger circuits because the highly conserved structure aids the incorporation of the large number of natural parts, these parts share phosphate as a common currency, each component may be connected to many others, and scaffolding can serve as modular, even dynamic, wires to connect components.

Natural systems have achieved powerful processing capabilities through the integration of transcriptional, translational, and posttranslational control. Building signaling systems from well-characterized, modular, independently tunable parts will facilitate rational and predictable design of novel signaling pathways and posttranslational control modules. Incorporating the posttranslational layers of control into genetic circuits will bring us closer to the ultimate goal of designing the complex regulatory networks necessary for adaptive behavior vital to living cells.

Materials and Methods

Strains and Plasmid Construction. The WW62 strain used in the experiments shown in Figs. 1–4 contains knockouts of OmpR, EnvZ, CpxR, CpxA, CusR, and CusS. WW62 was derived from BW27783 (43), an *E. coli* K12 strain, using standard procedures for creating markerless knockouts and P1 phage transduction. Plasmids were constructed with a hybrid BglBrick-derived (44) strategy. All expression levels were tuned with ribosome-binding site (RBS) libraries with degenerate oligo-nucleotide insertion. See *SI Materials and Methods* for detailed strain and plasmid construction methodology and for the process for incorporating autoinhibition into Taz.

Culture Method and Fluorescence Assays. Plasmids were transformed into the WW62 strain grown in Mops-rich defined medium (Teknova), and fluorescence and OD were measured at late log phase. Fluorescence per OD was normalized so that the cell autofluorescence equals 1 au. All error bars represent SE between experimental replicates performed on different days, each with at least three biological replicates. Experiments done with native TCSs present were transformed into BW27783. Minimal Mops medium was used to test aspartate induction. See *SI Materials and Methods* for details.

Estimating Relative Component Concentrations. Relative component concentrations were estimated from densitometry analysis of Western blots of with epitope-tagged components (Fig. S4). Experimental conditions were replicated, but with a C-terminal fusion of the triple FLAG tag epitope to one of the components to be quantified. Protein gels were run under standard conditions for NuPAGE 10% (wt/wt) Bis-Tris denaturing gels (Invitrogen) followed by transfer to nitrocellulose membrane and labeling with Sigma's monoclonal anti–FLAG M2-peroxidase (HRP) antibody using standard procedure. Western blots were exposed on an ImageQuant LAS 4000 (GE Healthcare), and densitometry analysis was performed on Image J analysis software (National Institutes of Health) to estimate relative component concentrations.

ACKNOWLEDGMENTS. We thank Michael Laub for plasmids used in preliminary work. This work was supported by funding from National Science Foundation (NSF) Synthetic Biology Engineering Research Center Grant EEC-0540879 and NSF Grant CBET-0756801.

1. Tamsir A, Tabor JJ, Voigt CA (2011) Robust multicellular computing using genetically encoded NOR gates and chemical 'wires' *Nature* 469(7329):212–215.
2. Friedland AE, et al. (2009) Synthetic gene networks that count. *Science* 324(5931): 1199–1202.
3. Basu S, Gerchman Y, Collins CH, Arnold FH, Weiss R (2005) A synthetic multicellular system for programmed pattern formation. *Nature* 434(7037):1130–1134.
4. Stricker J, et al. (2008) A fast, robust and tunable synthetic gene oscillator. *Nature* 456 (7221):516–519.
5. Lucks JB, Qi L, Whitaker WR, Arkin AP (2008) Toward scalable parts families for predictable design of biological circuits. *Curr Opin Microbiol* 11(6):567–573.
6. Bashor CJ, Helman NC, Yan S, Lim WA (2008) Using engineered scaffold interactions to reshape MAP kinase pathway signaling dynamics. *Science* 319(5869):1539–1543.
7. Dueber JE, Yeh BJ, Bhattacharyya RP, Lim WA (2004) Rewiring cell signaling: The logic and plasticity of eukaryotic protein circuitry. *Curr Opin Struct Biol* 14(6):690–699.
8. Dueber JE, Yeh BJ, Chak K, Lim WA (2003) Reprogramming control of an allosteric signaling switch through modular recombination. *Science* 301(5641):1904–1908.
9. Peisajovich SG, Garbarino JE, Wei P, Lim WA (2010) Rapid diversification of cell signaling phenotypes by modular domain recombination. *Science* 328(5976):368–372.
10. Bhattacharyya RP, Remenyi A, Yeh BJ, Lim WA (2006) Domains, motifs, and scaffolds: The role of modular interactions in the evolution and wiring of cell signaling circuits. *Annu Rev Biochem* 75:655–680.
11. Delebecque CJ, Lindner AB, Silver PA, Aldaye FA (2011) Organization of intracellular reactions with rationally designed RNA assemblies. *Science* 333(6041):470–474.
12. Moon TS, et al. (2011) Construction of a genetic multiplexer to toggle between chemosensory pathways in Escherichia coli. *J Mol Biol* 406(2):215–227.
13. Igo MM, Ninfa AJ, Stock JB, Silhavy TJ (1989) Phosphorylation and dephosphorylation of a bacterial transcriptional activator by a transmembrane receptor. *Genes Dev* 3(11): 1725–1734.
14. Yamada S, et al. (2006) The signaling pathway in histidine kinase and the response regulator complex revealed by X-ray crystallography and solution scattering. *J Mol Biol* 362(1):123–139.
15. Siryaporn A, Perchuk BS, Laub MT, Goulian M (2010) Evolving a robust signal transduction pathway from weak cross-talk. *Mol Syst Biol* 6:452.
16. Skerker JM, Prasol MS, Perchuk BS, Biondi EG, Laub MT (2005) Two-component signal transduction pathways regulating growth and cell cycle progression in a bacterium: A system-level analysis. *PLoS Biol* 3(10):e334.
17. Skerker JM, et al. (2008) Rewiring the specificity of two-component signal transduction systems. *Cell* 133(6):1043–1054.
18. Casino P, Rubio V, Marina A (2009) Structural insight into partner specificity and phosphoryl transfer in two-component signal transduction. *Cell* 139(2):325–336.
19. Yamamoto K, et al. (2005) Functional characterization in vitro of all two-component signal transduction systems from Escherichia coli. *J Biol Chem* 280(2):1448–1456.
20. Wise A, et al. (2010) The receiver domain of hybrid histidine kinase VirA: An enhancing factor for vir gene expression in Agrobacterium tumefaciens. *J Bacteriol* 192: 1534–1542.
21. Schmöe K, et al. (2011) Structural insights into Rcs phosphotransfer: The newly identified RcsD-ABL domain enhances interaction with the response regulator RcsB. *Structure* 19(4):577–587.
22. Jin T, Inouye M (1993) Ligand binding to the receptor domain regulates the ratio of kinase to phosphatase activities of the signaling domain of the hybrid Escherichia coli transmembrane receptor, Taz1. *J Mol Biol* 232(2):484–492.
23. Groban ES, Clarke EJ, Salis HM, Miller SM, Voigt CA (2009) Kinetic buffering of cross talk between bacterial two-component sensors. *J Mol Biol* 390(3):380–393.
24. Laub MT, Goulian M (2007) Specificity in two-component signal transduction pathways. *Annu Rev Genet* 41:121–145.
25. Siryaporn A, Goulian M (2008) Cross-talk suppression between the CpxA-CpxR and EnvZ-OmpR two-component systems in E. coli. *Mol Microbiol* 70(2):494–506.
26. Grünberg R, Ferrar TS, van der Sloot AM, Constante M, Serrano L (2010) Building blocks for protein interaction devices. *Nucleic Acids Res* 38(8):2645–2662.
27. Whitaker WR, Dueber JE (2011) Metabolic pathway flux enhancement by synthetic protein scaffolding. *Methods Enzymol* 497:447–468.
28. Posern G, et al. (1998) Development of highly selective SH3 binding peptides for Crk and CRKL which disrupt Crk-complexes with DOCK180, SoS and C3G. *Oncogene* 16 (15):1903–1912.
29. Dueber JE, Mirsky EA, Lim WA (2007) Engineering synthetic signaling proteins with ultrasensitive input/output control. *Nat Biotechnol* 25(6):660–662.
30. Dueber JE, et al. (2009) Synthetic protein scaffolds provide modular control over metabolic flux. *Nat Biotechnol* 27(8):753–759.
31. Thompson KE, Bashor CJ, Lim WA, Keating AE (2012) SYNZIP protein interaction toolbox: In vitro and in vivo specifications of heterospecific coiled-coil interaction domains. *ACS Synth Biol* 1:118–129.
32. Reinke AW, Grant RA, Keating AE (2010) A synthetic coiled-coil interactome provides heterospecific modules for molecular engineering. *J Am Chem Soc* 132(17):6025–6031.
33. Lohmueller JJ, Armel TZ, Silver PA (2012) A tunable zinc finger-based framework for Boolean logic computation in mammalian cells. *Nucleic Acids Res* 40(11):5180–5187.
34. Knudsen BS, et al. (1995) Affinity and specificity requirements for the first Src homology 3 domain of the Crk proteins. *EMBO J* 14(10):2191–2198.
35. Levchenko A, Bruck J, Sternberg PW (2000) Scaffold proteins may biphasically affect the levels of mitogen-activated protein kinase signaling and reduce its threshold properties. *Proc Natl Acad Sci USA* 97(11):5818–5823.
36. Chapman SA, Asthagiri AR (2009) Quantitative effect of scaffold abundance on signal propagation. *Mol Syst Biol* 5:313.
37. Batchelor E, Goulian M (2003) Robustness and the cycle of phosphorylation and dephosphorylation in a two-component regulatory system. *Proc Natl Acad Sci USA* 100 (2):691–696.
38. Rajakulendran T, Sahmi M, Lefrançois M, Sicheri F, Therrien M (2009) A dimerization-dependent mechanism drives RAF catalytic activation. *Nature* 461(7263):542–545.
39. Yeh BJ, Rutigliano RJ, Deb A, Bar-Sagi D, Lim WA (2007) Rewiring cellular morphology pathways with synthetic guanine nucleotide exchange factors. *Nature* 447(7144): 596–600.
40. Bhattacharyya RP, et al. (2006) The Ste5 scaffold allosterically modulates signaling output of the yeast mating pathway. *Science* 311(5762):822–826.
41. Capra EJ, et al. (2010) Systematic dissection and trajectory-scanning mutagenesis of the molecular interface that ensures specificity of two-component signaling pathways. *PLoS Genet* 6(11):e1001220.
42. Goulian M (2010) Two-component signaling circuit structure and properties. *Curr Opin Microbiol* 13(2):184–189.
43. Khlebnikov A, Datsenko KA, Skaug T, Wanner BL, Keasling JD (2001) Homogeneous expression of the P(BAD) promoter in Escherichia coli by constitutive expression of the low-affinity high-capacity AraE transporter. *Microbiology* 147(Pt 12):3241–3247.
44. Anderson JC, et al. (2010) BglBricks: A flexible standard for biological part assembly. *J Biol Eng* 4(1):1.
45. Kelley LA and Sternberg MJE (2009) *Nature Protocols* 4, 363–371.